Tailoring superconductivity with quantum dislocations

Mingda Li[1,2*], Qichen Song[1], Te-Huan Liu[1], Laureen Meroueh[1], Gerald D Mahan[3], Mildred S. Dresselhaus[4] and Gang Chen[1*]

[1]*Department of Mechanical Engineering, MIT, Cambridge, MA 02139, USA*
[2]*Department of Nuclear Science and Engineering, MIT, Cambridge, MA 02139, USA*
[3]*Department of Physics, Pennsylvania State University, Old Main, Stage College, PA16801, USA*
[4]*Department of Physics and Department of Electrical Engineering and Computer Sciences, MIT, Cambridge, MA 02139, USA*

*E-mail: mingda@mit.edu, *E-mail: gchen2@mit.edu

Abstract

Despite the established knowledge that crystal dislocations can affect a material's superconducting properties, the exact mechanism of the electron-dislocation interaction in a dislocated superconductor has long been missing. Being a type of defect, dislocations are expected to decrease a material's superconducting transition temperature (T_c) by breaking the coherence. Yet experimentally, even in isotropic type-I superconductors, dislocations can either decrease, increase or have little influence on T_c. These experimental findings have yet to be understood. Although the anisotropic pairing in dirty superconductors has explained impurity-induced T_c reduction, no quantitative agreement has been reached in the case a dislocation given its complexity. In this study, by generalizing the one-dimensional quantized dislocation field to three dimensions, we reveal that there are indeed two distinct types of electron-dislocation interactions. Besides the usual electron-dislocation potential scattering, there is another interaction driving an effective attraction between electrons that is caused by dislons, which are quantized modes of a dislocation. The role of dislocations to superconductivity is thus clarified as the competition between the classical and quantum effects, showing excellent agreement with existing experimental data. In particular, the existence of both classical and quantum effects provides a plausible explanation to the illusive origin of dislocation-induced superconductivity in semiconducting PbS/PbTe superlattice nanostructures. A quantitative criterion has been derived, in which a dislocated superconductor with low elastic moduli, small electron effective mass, and in a confined environment is inclined to enhance T_c. This provides a new pathway to engineer a material's superconducting properties by using dislocations as an additional degree of freedom.

Key Words: Dislocations; Electron-dislocation interaction; Dirty superconductor; Effective field theory.

Dislocations are irregular atomic position changes within regular ordering of atoms, extending along a line shape in a crystalline solid[1]. As a common type of line defect, the motion of a dislocation explains the large discrepancy between theoretical and experimental shear strengths in a crystal, and thereby leads

to plastic deformation behavior exhibited in materials[2]. In addition, dislocations have far-reaching impacts on material electronic properties, such as increasing electrical resistivity through deformation potential scattering[3] or Coulomb scattering[4] with electrons, changing electronic structures by forming electronic bound states[5] or low-dissipation conducting channels[6, 7], influencing superconducting properties[8, 9], etc.

Dislocations play a dual role in a material's superconducting properties. On the one hand, dislocations can immobilize the motion of a vortex line in type-II superconductors, leading to an increase of critical current. This mechanism is called flux pinning and is well understood[8, 9]. On the other hand, dislocations can change the superconducting transition temperature (T_c), a trend yet to be well understood. It is natural to consider that dislocations, as a type of material defect, can only cause a weakening of superconductivity since it results in electron scattering, and hence breaks the coherence of Cooper pairs. This picture is consistent with Anderson's theory of dirty superconductors[10], where T_c in a dirty superconductor is always slightly lower than the pure cases, and is even valid for high-temperature superconductors with anisotropic pairing[11]. However, experimentally, even in elementary type-I superconductors, the introduction of dislocations can either increase T_c (such as Zn), decrease T_c (such as Ti) or have negligible influence (such as Al) on T_c (listed in Table 1). This provides a hint that dislocations play a more profound role than behaving as mere impurities, yet no qualitative picture has been established to clarify its role, nor quantitative for that matter. A microscopic understanding of the electron-dislocation interaction mechanism in a dislocated superconductor has merit from not only a fundamental perspective, but also from a practical perspective, with the potential to provide guidelines for tailoring a material's superconducting properties through dislocations.

In this study, we show that the quantization of a dislocation itself, namely "dislon", is one suitable approach to tackle this problem. By generalizing the recently developed 1D dislon[12, 13] to 3D space, the resulting 3D dislon shows interesting statistics on its own, going beyond purely Bosonic or Fermionic behavior. This deviation is due to the topological definition of a crystal dislocation $\oint_C d\mathbf{u} = -\mathbf{b}$, where $\mathbf{u}$ is the lattice displacement field vector, $\mathbf{b}$ is the Burgers vector and C is an arbitrary loop enclosing the dislocation line[14]. To explore the significance of this quasiparticle, the electron-dislocation interaction is studied in the present work, where the electron effective Hamiltonian is obtained using a method inspired by the Faddeev-Popov gauge fixing approach[15, 16] to impose the dislocation's topological constraint. The effective electron Hamiltonian is shown to be composed of three terms - a diagonal quadratic term (non-interacting electron), an off-diagonal quadratic term (classical scattering which changes electron momentum) and a quartic term (quantum-mechanical interaction coupling two electrons). The elusive

role of the crystal dislocation on superconductivity is clarified as the competition between the two off-diagonal terms, where a generalized BCS gap equation incorporating both the classical and quantum interactions is derived. To validate the theory, the T_c of as many as ten dislocated superconductors are compared and excellent agreement is obtained. In particular, this theory provides a quantitative criteria for that which determines the change in T_c: a superconductor with low elastic moduli, small Burgers vector, high Poisson ratio, small effective mass, high Debye frequency and high density of state at the Fermi level. Most importantly, in a confined environment, such a superconductor tends to exhibit an increase in T_c when dislocations are introduced. Our theory provides a plausible explanation to the mysterious origin of the dislocation induced superconductivity in PbTe/PbS superlattice at nanoscale.

The foundation of a quantized dislocation

The best way to understand the quantized dislocation is most easily done by comparing it with a phonon. A phonon is a quantized lattice wave which can be mode-expanded in terms of plane waves[17]:

$$\mathbf{u}^{ph}(\mathbf{R}) = \frac{1}{\sqrt{N}} \sum_{\mathbf{k}} u_{\mathbf{k}}^{ph} \boldsymbol{\varepsilon}_{\mathbf{k}\lambda} e^{i\mathbf{k}\cdot\mathbf{R}} \tag{1}$$

where $\mathbf{u}^{ph}$ is the lattice displacement at a given spatial position $\mathbf{R}$, i.e. the difference of the atomic position with and without the presence of phonon induced atomic position deviations, $\boldsymbol{\varepsilon}_{\mathbf{k}\lambda}$ is the polarization vector and $u_{\mathbf{k}}^{ph}$ is the lattice displacement in the $\mathbf{k}$-component mode, and $\mathbf{k}$ is a 3D vector in reciprocal space. In the static limit, there is no displacement, i.e. $u_{\mathbf{k}}^{ph} = 0$. As for a dislocation, inspired by mode-expansion work in 1D[12, 13], we expand the lattice displacement vector caused by a single dislocation line $\mathbf{u}(\mathbf{R})$ extending along the *z*-direction with core position $(x_0, y_0) = (0,0)$ as (Supporting Information I)

$$\mathbf{u}(\mathbf{R}) = \frac{1}{A} \sum_{\mathbf{k}} \mathbf{F}(\mathbf{k}) e^{i\mathbf{k}\cdot\mathbf{R}} u_{\mathbf{k}} \tag{2}$$

where A is the sample area, $u_{\mathbf{k}}$ is the dimensionless displacement, and $\mathbf{F}(\mathbf{k})$ is an expansion function. For later convenience we use $\mathbf{s}$ to denote the 2D momentum perpendicular to the dislocation direction ($\mathbf{s} \equiv (k_x, k_y)$), and κ as the momentum along the dislocation direction, i.e. $\mathbf{k} \equiv (k_x, k_y, k_z) \equiv (\mathbf{s}, \kappa)$. In other words, instead of a plane-wave expansion, here it is a localized mode expansion around the dislocation core. A schematic is shown in Fig. S1. in Supporting Information I. Unlike the phonon case where $\mathbf{k}$ is a good quantum number due to translational symmetry, here k is more like a complete set for mode expansion and the local modes $\mathbf{F}(\mathbf{k})$ are not necessarily orthogonal to each other, but must be compatible

with a classical dislocation without quantum fluctuations. In a 3D isotropic solid, for a dislocation line along the z-direction and glide plane within the *xz*-plane, $F_i(\mathbf{k})$ can be written explicitly as (Supporting information I)

$$\mathbf{F}(\mathbf{k}) \equiv \mathbf{F}(\mathbf{s};\kappa) = +\frac{1}{k_x k^2}\left(\mathbf{n}(\mathbf{b}\cdot\mathbf{k}) + \mathbf{b}(\mathbf{n}\cdot\mathbf{k}) - \frac{1}{(1-\nu)}\frac{\mathbf{k}(\mathbf{n}\cdot\mathbf{k})(\mathbf{b}\cdot\mathbf{k})}{k^2}\right) \tag{3}$$

where **n** is the glide plane normal direction, **b** is the Burgers vector, and ν is the Poisson ratio. The reason for the specific form in Eq. (2) and (3) is straightforward, such that under the following boundary condition,

$$\lim_{\kappa\to 0} u_{\mathbf{k}} = 1, \text{ for } \forall \mathbf{s} \tag{4}$$

Eq. (2) reduces to the static, quenched dislocation, for both edge and screw dislocations (Supporting information I). In fact, Eq. (4) – the reducibility to a classical dislocation without quantum fluctuation– can be considered as the starting point of this theory.

A brief comparison of a phonon and a quantized dislocation (aka dislon) is provided in Table 1.

The 3D dislon Hamiltonian

By substituting the dislocation's displacement vector **u**(**R**) in Eq. (2) into a classical Hamiltonian composed of kinetic energy $T = \frac{\rho}{2}\int \sum_{i=1}^{3} \dot{\mathbf{u}}_i^2(\mathbf{R}) d^3\mathbf{R}$ and potential energy $U = \frac{1}{2}\int c_{ijkl} u_{ij} u_{kl} d^3\mathbf{R}$, where ρ is the mass density, c_{ijkl} is the stiffness tensor and u_{ij} is the strain tensor, the classical dislocation's Hamiltonian $H = T + U$ can be rewritten as (Supporting Information II)

$$H = \sum_{\mathbf{k}} \frac{p_{\mathbf{k}} p_{-\mathbf{k}}}{2m_{\mathbf{k}}} + \sum_{\mathbf{k}} \frac{m_{\mathbf{k}}\Omega_{\mathbf{k}}^2}{2} u_{\mathbf{k}} u_{-\mathbf{k}} \tag{5}$$

where $m_{\mathbf{k}} \equiv \rho\left|\mathbf{F}(\mathbf{k})\right|^2 / L$ is a mass-like coefficient in which L is the system size assuming that the dislocation is located in an isotropic solid with box length L, $p_{\mathbf{k}} = m_{\mathbf{k}}\dot{u}_{-\mathbf{k}}$ is the canonical momentum conjugate to $u_{\mathbf{k}}$, $\Omega_{\mathbf{k}} \equiv \sqrt{\left[(\lambda+\mu)[\mathbf{k}\cdot\mathbf{F}(\mathbf{k})]^2 + \mu k^2\left|F(\mathbf{k})\right|^2\right] / \rho\left|F(\mathbf{k})\right|^2}$ plays the role of an excitation, in which we have assumed an isotropic solid hence $c_{ijkl} = \lambda\delta_{ij}\delta_{kl} + \mu(\delta_{ik}\delta_{jl} + \delta_{il}\delta_{jk})$, with λ the Lamé's first parameter and μ the shear modulus.

The form of. Eq. (5) appears to be similar to the case of the phonon, but with a momentum-dependent mass term. However, there is a huge difference due to the topological constraint set by Eq. (4). Defining $Z_{\mathbf{k}} \equiv \sqrt{\hbar/2m_{\mathbf{k}}\Omega_{\mathbf{k}}}$, if we impose a canonical quantization procedure such that

$$\begin{cases} u_{\mathbf{k}} = Z_{\mathbf{k}}\left[a_{\mathbf{k}} + a_{-\mathbf{k}}^{+}\right] \\ p_{\mathbf{k}} = \dfrac{i\hbar}{2Z_{\mathbf{k}}}\left[a_{\mathbf{k}}^{+} - a_{-\mathbf{k}}\right] \end{cases} \tag{6}$$

it can be proven that the usual Bosonic canonical commutation relation $[a_{\mathbf{k}}, a_{\mathbf{k}'}^{+}] = \delta_{\mathbf{k}\mathbf{k}'}$ is indeed incompatible with the boundary condition of Eq. (4), yet compatible with the following quantization condition (Supporting Information III)

$$[a_{\mathbf{k}}, a_{\mathbf{k}'}^{+}] = \delta_{\mathbf{k}\mathbf{k}'}\,\mathrm{sgn}(\mathbf{k}) \tag{7}$$

where $\mathrm{sgn}(\mathbf{k})$ is the vector sign function. A few properties related to vector sign functions are discussed in Supporting Information IV.

It is well known that a constraint may result in a breakdown of a canonical quantization condition[18]. For instance, dimensional constraint leads to anyonic statistics[19]. Here, the dislocation's constraint is also shown to be incompatible with canonical quantization condition, as shown in Eq. (7).

In other words, the topological constraint of the dislocation given by Eq. (4) prevents the quantized displacement field of a dislocation from being purely Bosonic. To understand this, we define a new operator $b_{-\mathbf{k}}^{+} = a_{\mathbf{k}}$ whenever $\mathrm{sgn}(\mathbf{k}) < 0$, hence the new fields $b_{\mathbf{k}}$ and $b_{\mathbf{k}}^{+}$ satisfy canonical quantization condition $[b_{\mathbf{k}}, b_{\mathbf{k}'}^{+}] = \delta_{\mathbf{k}\mathbf{k}'}$ (Supporting Information V). Therefore, the quantized Hamiltonian can finally be written as two Bosonic fields ***a*** and ***b*** (Supporting Information V)

$$H = \sum_{\mathbf{k}} \hbar\Omega(\mathbf{k}) a_{\mathbf{k}}^{+} a_{\mathbf{k}} = \sum_{\mathbf{k}\geq 0} \hbar\Omega(\mathbf{k})\left(a_{\mathbf{k}}^{+} a_{\mathbf{k}} + \frac{1}{2}\right) + \sum_{\mathbf{k}\geq 0} \hbar\Omega(\mathbf{k})\left(b_{\mathbf{k}}^{+} b_{\mathbf{k}} + \frac{1}{2}\right) \tag{8}$$

where we have used the fact that $\Omega(\mathbf{k} = \mathbf{0}) = 0$, and the short-hand notation of $\mathbf{k} \geq 0$ denoting $\mathrm{sgn}\,\mathbf{k} \geq 0$. The necessity of two fields in representing a quantized dislocation very much resembles a Dirac monopole[20], where two magnetic vector potentials have to be defined for the south and north poles.. In both cases, a single field quantity – whether a classical vector potential or a quantized Bosonic field – is simply not sufficient in describing the topological nature.

The electron-dislon interaction

The generic electron-ion interacting Hamiltonian can be represented using the deformation potential approximation as[17]

$$H_{e-ion} = \int d^3\mathbf{R}\rho_e(\mathbf{R})\sum_{j=1}^{N}\nabla_{\mathbf{R}}V_{ei}(\mathbf{R}-\mathbf{R}_j^0)\cdot\mathbf{u}_j \tag{9}$$

where $\rho_e(\mathbf{R})$ is the charge density operator which is defined as $\rho_e(\mathbf{R}) = en_e(\mathbf{R}) = \frac{e}{V}\sum_{\mathbf{kp}\sigma} e^{-i\mathbf{p}\cdot\mathbf{R}}c^+_{\mathbf{k}+\mathbf{p}\sigma}c_{\mathbf{k}\sigma}$, and the Coulomb potential $V_{ei}(\mathbf{R}-\mathbf{R}_j^0) = \frac{1}{V}\sum_{\mathbf{k}} V_{\mathbf{k}}e^{i\mathbf{k}\cdot(\mathbf{R}-\mathbf{R}_j^0)}$, having a Fourier component $V_{\mathbf{k}} \equiv \frac{4\pi Ze}{k^2+k_{TF}^2}$, in which k_{TF} is the Thomas-Fermi screening wavenumber. Using Eq. (2), the electron-quantized dislocation (aka dislon) interacting Hamiltonian Eq. (9) can be further simplified as (Supporting information VI)

$$H_{e-dis} = \sum_{\substack{\mathbf{k}'\sigma\\ \mathbf{k}\geq 0}} g_{\mathbf{k}}c^+_{\mathbf{k}'+\mathbf{k}\sigma}c_{\mathbf{k}'\sigma}(a_{\mathbf{k}}+b_{\mathbf{k}}) + \sum_{\substack{\mathbf{k}'\sigma\\ \mathbf{k}\geq 0}} g^*_{\mathbf{k}}c^+_{\mathbf{k}'-\mathbf{k}\sigma}c_{\mathbf{k}'\sigma}(b^+_{\mathbf{k}}+a^+_{\mathbf{k}}) \tag{10}$$

in which the electron-dislocation coupling constant is defined as $g_{\mathbf{k}} \equiv \frac{eN}{VA}\sqrt{N_D}V_{\mathbf{k}}\left[i\mathbf{k}\cdot\mathbf{F}(\mathbf{k})\right]\sqrt{\frac{\hbar}{2m_{\mathbf{k}}\Omega_{\mathbf{k}}}}$

where N is the number of ions in the system, V is the sample volume, and N_D is the number of dislocations (Supporting Information VII). A brief comparison of an electron-phonon vs electron-dislon interaction is also provided in Supporting Information VII.

Effective field theory of electrons

To see how the electron-dislon interaction of Eq. (10) under the constraint of Eq. (4) really affects material electronic properties, we adopt a functional integral approach[21] to eliminate the dislon degree of freedom and establish an effective field theory for solely electrons. The benefit of this approach is that the constraint of Eq. (4) can be properly taken into account. The effective electron Hamiltonian can finally be written as (Supporting Information VIII)

$$\begin{aligned} H_{eff} &= H_0 + H_c + H_q \\ &= \sum_{\mathbf{k}\sigma}\left(\varepsilon_{\mathbf{k}}-\mu\right)c^+_{\mathbf{k}\sigma}c_{\mathbf{k}\sigma} + \sum_{\mathbf{k}\sigma}\sum_{\mathbf{s}}\left(A_{\mathbf{s}}c^+_{\mathbf{k}+\mathbf{s}\sigma} + A^*_{\mathbf{s}}c^+_{\mathbf{k}-\mathbf{s}\sigma}\right)c_{\mathbf{k}\sigma} + \sum_{\mathbf{qkk}'}V_{eff}(\mathbf{q})c^+_{\mathbf{k}+\mathbf{q}\uparrow}c^+_{-\mathbf{k}\downarrow}c_{-\mathbf{k}'+\mathbf{q}\downarrow}c_{\mathbf{k}'\downarrow} \end{aligned} \tag{11}$$

in which $\varepsilon_{\mathbf{k}}$ is the single-electron energy and μ is the Fermi level. The classical electron-dislocation scattering H_c (Figure 1a green straight line) indicates a change of electron momentum perpendicular to

the dislocation line direction (since **s** is the 2D momentum perpendicular to the dislocation direction), with scattering amplitude $A_{\mathbf{s}} = \frac{eN}{2VA}\sqrt{N_{dis}}V_{\mathbf{s}}\left[i\mathbf{s}\cdot\mathbf{F}(\mathbf{s})\right]$. It can also be shown that the scattering amplitude $A_{\mathbf{s}}$ is reducible to the classical dislocation deformation scattering potential[22], where $\delta V = -\frac{a_c b}{2\pi}\left(\frac{1-2\nu}{1-\nu}\right)\frac{\sin\theta}{r}$, supporting the consistency of the present theory (Supporting Information IX). In addition, the relaxation rate $\Gamma_{\mathbf{k}}$ of classical scattering is fully consistent with semi-classical theory, $\Gamma \propto n_{dis}b^2\left(\frac{1-2\nu}{1-\nu}\right)^2$ (Supporting Information X). Furthermore, the term $V_{eff}(\mathbf{q}) = -\frac{\hbar\Omega_{\mathbf{q}}g_{\mathbf{q}}^{*}g_{\mathbf{q}}}{-\omega^2+\hbar^2\Omega_{\mathbf{q}}^2}$ indicates an effective attraction between electrons pairs (Figure 1a wavy line). Eq. (11) is the main result of this study, describing how dislocations will interact with electrons from a quantitative many-body viewpoint. Interestingly, the effective attraction interaction mediated by a dislon shares some structural similarity with the interaction mediated by a phonon[23], which leads to phonon-mediated superconductivity. Here the interaction has a different coupling constant and the phonon dispersion $\omega_{\mathbf{q}}$ is replaced by dislon dispersion $\Omega_{\mathbf{q}}$, as shown in Table 1.

The influence of dislocations to superconducting transition temperature

Now using the effective electron Hamiltonian of an electron-dislon interaction (Eq. (11)), and incorporating the effective electron Hamiltonian from electron-phonon coupling, a generalized BCS equation taking into account both dislocations and phonons is derived using an auxiliary field approach[24] , which is capable of computing the influence of a dislocation upon the superconducting transition temperature (Supporting information XI)

$$\frac{1}{g_{ph}+g_{dis}} = N(\mu)\int_0^{\omega_D}\frac{\tanh\left(\frac{\xi+\Gamma+i\Gamma}{2T_c}\right)+\tanh\left(\frac{\xi+\Gamma-i\Gamma}{2T_c}\right)}{2\left(\xi+\Gamma\right)}d\xi \tag{12}$$

where g_{ph} is the electron-phonon coupling constant in usual BCS theory, which is measurable or computable from packages like EPW[25], ω_D is the Debye frequency, and $N(\mu)$ is the density of states at the Fermi level. In particular, g_{dis} is the effective electron-dislon coupling constant, which can be written as (Supporting Information XI)

$$g_{dis} = -\left(\frac{N}{V}\right)^2 \frac{n_{dis}}{L} \frac{\left(4\pi Ze^2\right)^2}{2k_{TF}^4\left(\lambda+2\mu\right)} \tag{13}$$

where k_{TF} is the Thomas-Fermi screening wavevector. Since we are interested in electrons near the Fermi level and $\omega_D \ll \mu$, and the decay mainly exists near the Fermi level, we write the classical decay constant as (Supporting Information X)

$$\Gamma \sim \Gamma_{k_F} = \frac{\pi m^*}{4\hbar^2 k_F^2 k_{TF}^4}\left(\frac{Ze^2N}{V}\right)^2 n_{dis} b^2 \left(\frac{1-2\nu}{1-\nu}\right)^2 \tag{14}$$

where m^* is the effective electron mass, and k_F is the Fermi wavevector.

From Eq. (12)-(14), the role of a dislocation to a material's superconductivity becomes clear: it is governed by the competition between the classical scattering Γ and the quantum interaction g_{dis} (Figure 1b). It also becomes clear that if the quantum interaction dominates $g_{dis}/g_{ph} \gg \Gamma/\omega_D$, the superconducting transition temperature T_c increases compared to a pure crystal, and vice versa. In particular, the near-linearity of the $T_c = T_c^0$ curve (black-dotted line) indicates the possibility of using a single parameter, namely the quantum-to-classical ratio

$$\frac{Quantum}{Classical} \sim \frac{g_{dis}/g_{ph}}{\Gamma/\omega_D} \sim \frac{32\pi\hbar^2 k_F^2\left(\frac{1-\nu}{1-2\nu}\right)^2}{m^* b^2\left(\lambda+2\mu\right)L} \frac{\omega_D N(\mu)}{\left[N(\mu)g_{ph}\right]} \tag{15}$$

to estimate whether the presence of the dislocation will increase or decrease T_c. The reason we use the ratio Eq. (15) as an indicator is that the n_{dis} dependence is cancelled out in Eq. (15), a quantity not measured in many experimental reports. In addition, as shown in Fig. 1b, along the dashed line, $T_c = T_c^0$ regardless of n_{dis}, further validating the use of Eq. (15). Therefore, we conclude that for a possible increase of T_c, it is preferable for a material to have a small electron effective mass m^*, low values of rigidity λ and μ, and a smaller system size *L*. What is striking from Eq. (15) is that a combination of electronic properties and material properties, which are generally considered independent, appear to coordinate together to determine the superconducting properties.

Comparison with Existing Experimental Data

Now we are ready to compare the theory Eqs. (12) and (15) with existing experimental data. In fact, the advantage of Eq. (15) is quite straightforward, since the dislocation density n_{dis} - which is required to compute the absolute magnitude of g_{dis} and Γ but is often missing due to the paucity of experimental data- is cancelled out and does not appear in Eq. (15) (See Methods). We see that even when relying on the simplified expression of g_{dis} and Γ as in Eqs. (13) and (14), the predicted T_c show excellent quantitative agreement with existing experimental data (Table 2).

In addition to the small influences of dislocations on superconductivity, it is worth mentioning that in some semiconducting monochalgogenide nanostructures[26, 27] such as PbTe/PbS superlattice, introducing high-density misfit dislocations could directly drive a semiconductor-superconductor phase transition. Although some qualitative explanation of the pressure-induced phase transition or dislocation-induced flat band[28] have been given, no quantitative agreement has been reached. Here we show that the present theory, even though it is formulated for an isotropic system, can still explain the magnitude of the T_c change observed in experiments. For a PbTe/PbS superlattice, due to its very low elastic moduli[29] ($\lambda = 19.9\text{GPa}$, $\mu = 21.4\text{GPa}$), very small effective mass[30] ($m^* \sim 0.02m_e$ in PbTe), small dislocation grid period ($L = 5.2\text{nm}$ in PbTe/PbS, where we have assumed that the system size is the dislocation grid size)[26], and high electron density of state caused by the formation of flat band[28], the estimated quantum-to-classical ratio according to Eq. (15) is expected to be exceedingly high, leading to a great enhancement of superconducting transition temperature T_c. Assuming a 136K Debye temperature (which is the Debye temperature of pure PbTe) and $N(\mu)g_{ph} = 0.1$ without dislocations, the resulting dislocation-free superconducting transition temperature gives only $T_c^0 < 0.01\text{K}$. When dislocations are introduced, assuming $N(\mu)g_{ph} = 0.2$ due to the increase in the density of states caused by the electronic flat band[28], the resulting T_c could be increased to ~10K, as shown in Fig. 2b. This is in excellent agreement with a series of semiconducting monochalgogenide nanostructures with different dislocation grid periods, hence different system sizes, where both theory and experiments reveal a common feature: a larger size gives a lower T_c. In addition, the experiments showed that both YbS/YbSe and YbS/EuS superlattices are not superconducting, while PbSe/EuS, PbS/YbS and PbTe/YbS are superconductors. From the present theory, we could understand this readily: there has to be a narrow bandgap semiconductor to reduce the m^* and hence increase the quantum to classical ratio in Eq. (15), in order to allow for superconductivity. Since both YbS and EuS are large bandgap insulators which in general have a larger effective mass compared with narrow bandgap semiconductors such as PbTe[31] (for instance $m^*(\text{EuS}) = 0.45m_e$ [32]), the quantum-

to-classical ratio is greatly reduced. The existence of superconductivity in YbS/EuS further excludes the dominating role of ferromagnetism in EuS. This provides a possible working theory to explain the effect of dislocations on materials superconductivity.

Conclusions

In this study, we show that due to a dislocation's topological constraint as given in Eq. (4), a quantized dislocation, the "dislon", is indeed composed of two Bosonic fields (8). As a result, we show that there are two distinct types of electron-dislocation interactions: besides the well-known classical scattering where electron momentum is changed, a new type of interaction is revealed, which could couple electron pairs through a dislon (Eq. (11)). This leads to the resolution in understanding the role of dislocations in a materials superconducting transition temperature T_c . Ultimately, the competition between two interactions determines the direction of change in T_c. The theory not only shows very good agreement with multiple previous experiments in elementary BCS superconductors, but also explains the mystic phenomena of why misfit dislocations in a superlattice system could turn a semiconductor into a superconductor. This theory may open up new routes to understanding the role of dislocations on material electronic, thermal, magnetic and optical properties at a new level of clarity.

Methods

Experimental Data

Simple material data for metals are taken from the Landolt–Börnstein database[33] and a few others[34-36] to ensure consistency, while the data for dislocated superconductors are taken separately[37-42], which are all compiled in the Table in Supporting Information XII. Since the dislocation density is unknown for the majority of materials, and the ratio in Eq. (15) does not fix the absolute magnitude of g_{dis} , we have chosen a reasonably estimated value $g_{dis} = 0.02 g_{ph}$ to scale all materials (as an example, take dislocation density $n_D \sim 10^{12} cm^{-2}$, $L = 10nm$ and other values from Zn, $\frac{g_{dis}}{g_{ph}} \sim \left(\frac{N}{V}\right)^2 \frac{n_{dis}}{L} \frac{\left(4\pi Ze^2\right)^2}{2k_{TF}^4\left(\lambda + 2\mu\right)}$). A different choice of parameters within a reasonable range would slightly change the magnitude but not qualitatively change the behavior. Since g_{dis} and Γ have different dimensions, for computational purposes we normalize $g_{dis} \to g_{dis}/V$ to match experimental energy dimensions so that all coupling strengths have the dimension

of energy. To estimate the Fermi-wavevector using the free-electron model, we use $k_F = \left(\frac{9\pi}{4}\right)^{1/3} \frac{1}{a_0 r_s}$,

where the density parameter is defined as $\frac{4\pi}{3} n a_0^3 r_s^3 \equiv 1$.

References

1. Hirth, J. P.; Lothe, J., *Theory of dislocations*. 2nd ed.; Krieger Pub. Co.: Malabar, FL, 1992; p xii, 857 p.
2. Hull, D.; Bacon, D. J., *Introduction to dislocations*. 4th ed.; Butterworth-Heinemann: Oxford Oxfordshire ; Boston, 2001; p vii, 242 p.
3. Dexter, D. L.; Seitz, F. *Phys Rev* **1952,** 86, (6), 964-965.
4. Jena, D.; Gossard, A. C.; Mishra, U. K. *Appl Phys Lett* **2000,** 76, (13), 1707.
5. Landauer, R. *Phys Rev* **1954,** 94, (5), 1386-1388.
6. Ran, Y.; Zhang, Y.; Vishwanath, A. *Nat Phys* **2009,** 5, (4), 298-303.
7. Reiche, M.; Kittler, M.; Erfurth, W.; Pippel, E.; Sklarek, K.; Blumtritt, H.; Haehnel, A.; Uebensee, H. *J Appl Phys* **2014,** 115, (19).
8. Larkin, A. I.; Ovchinnikov, Y. N. *J Low Temp Phys* **1979,** 34, (3), 409-428.
9. Dewhughe.D. *Philosophical Magazine* **1974,** 30, (2), 293-305.
10. Anderson, P. W. *J Phys Chem Solids* **1959,** 11, (1-2), 26-30.
11. Radtke, R. J.; Levin, K.; Schuttler, H. B.; Norman, M. R. *Physical Review B* **1993,** 48, (1), 653-656.
12. Li, M.; Cui, W.; Dresselhaus, M. S.; Chen, G. *New Journal of Physics* **2017,** 19, (1), 013033.
13. Li, M.; Ding, Z.; Meng, Q.; Zhou, J.; Zhu, Y.; Liu, H.; Dresselhaus, M. S.; Chen, G. *Nano Letters* **2017,** 15, 1587.
14. Nabarro, F. R. N., *Theory of crystal dislocations*. Dover Publications: New York, 1987; p xvii, 821 p.
15. Faddeev, L. D.; Popov, V. N. *Physics Letters B* **1967,** 25, (1), 29-30.
16. Gribov, V. N. *Nucl Phys B* **1978,** 139, (1-2), 1-19.
17. Bruus, H.; Flensberg, K., *Many-body quantum theory in condensed matter physics : an introduction*. Oxford University Press: Oxford ; New York, 2004; p xix, 435 p.
18. Kleinert, H., *Path integrals in quantum mechanics, statistics, polymer physics, and financial markets*. 5th ed.; World Scientific: New Jersey, 2009; p xliii,1579 p.
19. Nayak, C.; Simon, S. H.; Stern, A.; Freedman, M.; Das Sarma, S. *Rev Mod Phys* **2008,** 80, (3), 1083-1159.
20. Nakahara, M., *Geometry, topology, and physics*. 2nd ed.; Institute of Physics Publishing: Bristol ; Philadelphia, 2003; p xxii, 573 p.
21. Negele, J. W.; Orland, H., *Quantum many-particle systems*. Addison-Wesley Pub. Co.: Redwood City, Calif., 1988; p xviii, 459 p.
22. Wood, C. E. C.; Jena, D., *Polarization effects in semiconductors : from ab initio theory to device application*. Springer: New York, 2008; p xiii, 515 p.
23. Aynajian, P., *Electron-phonon interaction in conventional and unconventional superconductors*. Springer: Heidelberg ; New York, 2010; p xii, 101 p.
24. Nagaosa, N., *Quantum field theory in condensed matter physics*. Springer: Berlin ; New York, 1999; p x, 206 p.
25. Poncé, S.; Margine, E. R.; Verdi, C.; Giustino, F. *Computer Physics Communications* **2016,** 209, 116-133.
26. Fogel, N. Y.; Buchstab, E. I.; Bomze, Y. V.; Yuzephovich, O. I.; Sipatov, A. Y.; Pashitskii, E. A.; Danilov, A.; Langer, V.; Shekhter, R. I.; Jonson, M. *Physical Review B* **2002,** 66, (17), 174513.
27. Fogel, N. Y.; Pokhila, A. S.; Bomze, Y. V.; Sipatov, A. Y.; Fedorenko, A. I.; Shekhter, R. I. *Physical Review Letters* **2001,** 86, (3), 512-515.
28. Tang, E.; Fu, L. *Nat Phys* **2014,** 10, (12), 964-969.
29. Ni, J. E.; Case, E. D.; Khabir, K. N.; Stewart, R. C.; Wu, C. I.; Hogan, T. P.; Timm, E. J.; Girard, S. N.; Kanatzidis, M. G. *Mater Sci Eng B-Adv* **2010,** 170, (1-3), 58-66.
30. Lead telluride (PbTe) effective masses. In *Non-Tetrahedrally Bonded Elements and Binary Compounds I*, Madelung, O.; Rössler, U.; Schulz, M., Eds. Springer Berlin Heidelberg: Berlin, Heidelberg, 1998; pp 1-3.
31. Chu, J.; Sher, A., *Physics and properties of narrow gap semiconductors*. Springer: New York, 2008; p xii, 605 p.
32. Cho, S. J. *Physical Review B* **1970,** 1, (12), 4589-4603.
33. *The Landolt-Börnstein Database*, Springer-Verlag Berlin Heidelberg & Material Phases Data System (MPDS): 2014.
34. Morel, P.; Anderson, P. W. *Phys Rev* **1962,** 125, (4), 1263-1271.
35. Visscher, P. B.; Falicov, L. M. *Phys Status Solidi B* **1972,** 54, (1), 9-51.
36. Rose, J. H.; Shore, H. B. *Physical Review B* **1993,** 48, (24), 18254-18256.

37. Joiner, W. C. H. *Phys Rev* **1965,** 137, (1A), A112-A118.
38. Steele, M. C.; Hein, R. A. *Phys Rev* **1953,** 91, (2), 490-490.
39. von Minnigerode, G. *Zeitschrift für Physik* **1959,** 154, (4), 442-459.
40. Schenck, J. F.; Shaw, R. W. *J Appl Phys* **1969,** 40, (13), 5165-&.
41. Krah, W.; Kohnlein, D. *Z Phys B Con Mat* **1977,** 28, (1), 19-22.
42. Köhnlein, D. *Zeitschrift für Physik* **1968,** 208, (2), 142-158.

Acknowledgements

ML would thank H. Liu, R. Jaffe, O. Yuzephovich, J. Synder, L. Fu, and R. Hanus for their helpful discussions. ML, QS, MSD and GC would like to thank support by S^3TEC, an Energy Frontier Research Center funded by U.S. Department of Energy (DOE), Office of Basic Energy Sciences (BES) under Award No. DE-SC0001299/DE-FG02-09ER46577 (for fundamental research on electron phonon interaction in thermoelectric materials) and by Defense Advanced Research Projects Agency (DARPA) MATRIX program HR0011-16-2-0041 (for developing and applying the simulation codes).

Additional information

Supplementary information is available in the online version of the paper. Reprints and permissions information is available online. Correspondence and requests for materials should be addressed to ML (mingda@mit.edu) or GC (gchen2@mit.edu).

Competing financial interests

The authors declare no competing financial interests.

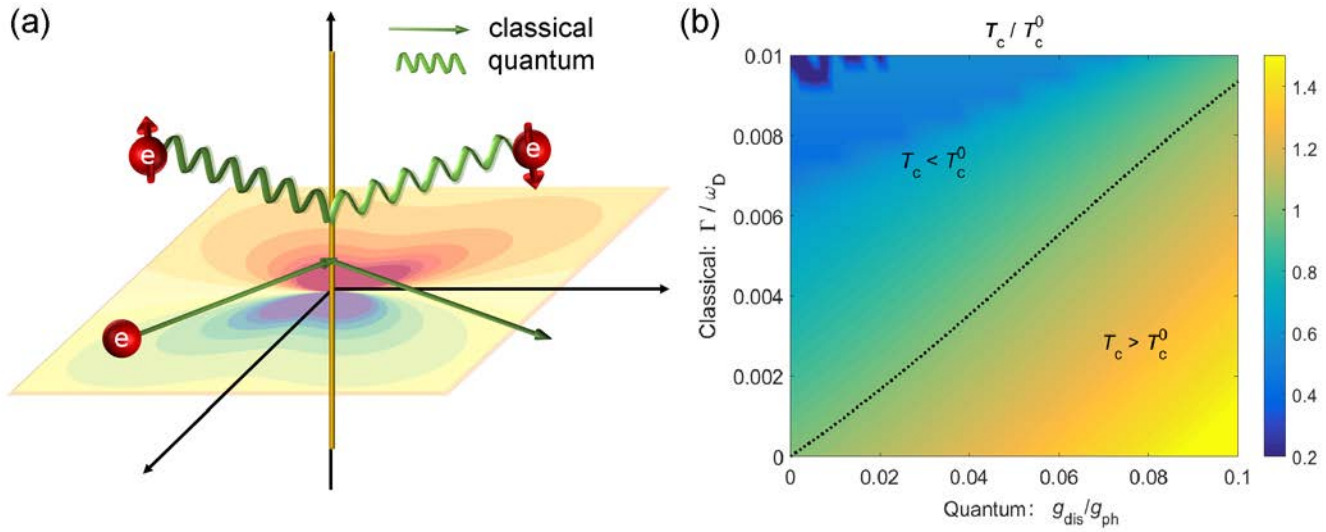

Figure 1. Classical vs quantized dislocation. (a) The electron-dislocation interactions have two types. The classical interaction (green straight lines with arrows) denotes the momentum-transfer scattering resulting in a weakened superconductivity, while another quantum interaction (green wavy lines) leads to an effective attraction between electrons, resulting in enhanced superconductivity. (b) The influence of a dislocation to a materials superconducting transition temperature T_c is explained as the competition between classical and quantum interactions. There is a clear line (black-dotted) separating the dislocation-enhanced superconductivity ($T_c > T_c^0$) region from the dislocation-weakened superconductivity ($T_c < T_c^0$) region.

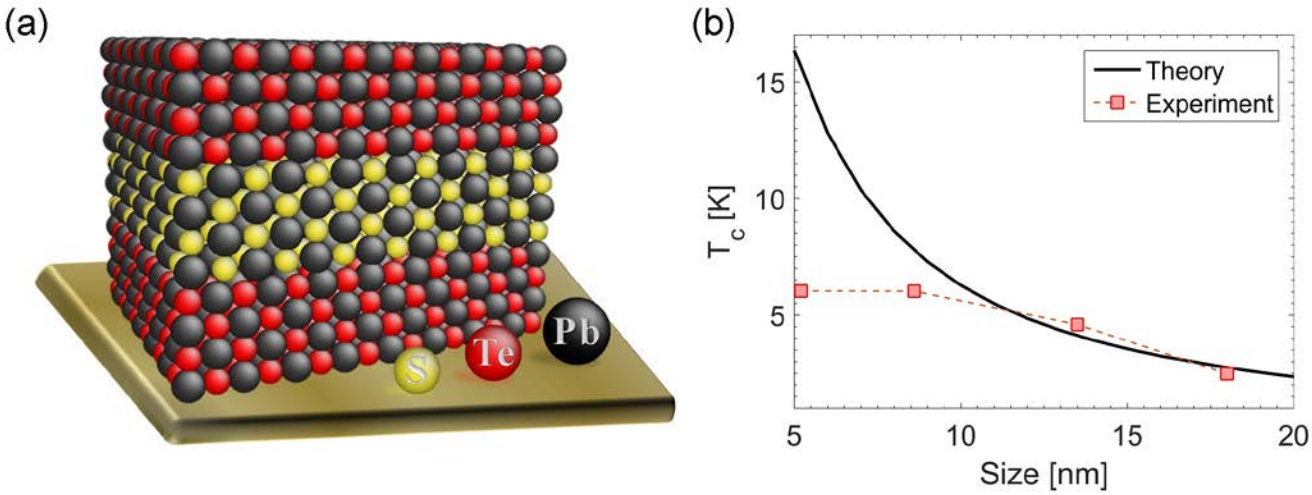

Figure 2. Dislocation induced superconductivity in semiconducting monochalgogenide superlattice. (a) Atomic configuration of a PbTe/PbS superlattice. When misfit dislocations are introduced, the semiconducting superlattice system experiences a phase transition, thus becoming a superconductor. (b)The comparison between the present theory using Eqs. (12)–(15) with PbTe/PbS and pure PbTe parameters (see main text), and the experimental reports[26], where the four data points correspond to PbTe/PbS, PbTe/PbSe, PbS/PbSe and PbSe/EuS,

with the system size $L = 5.2\text{nm},\ 8.6\text{nm},\ 13.5\text{nm}$ and 18.0nm, respectively. Both theory and experiments show the same trend that is a larger size leads to a reduced superconducting transition temperature T_c .

Table 1. Comparison between theory and experimental superconducting transition temperature for a series of simple-metal dislocated superconductors, showing good agreement. The parameters used for calculation and the corresponding references are listed in Supporting Information XII.

	Al	**In**	**Nb**	**Pb**	**Sn**	**Ta**	**Ti**	**Tl**	**V**	**Zn**
$\left[T_c/T_c^0\right]_{\text{Exp}}$	1.00	1.04	1.06	1.00	1.06	1.00	0.75	1.13	1.09	1.54
$\left[T_c/T_c^0\right]_{\text{Theory}}$	0.94	1.07	1.06	1.03	1.06	1.01	0.87	1.07	1.05	1.28
[Trend]$_{\text{Exp}}$	—	↑	↑	—	↑	—	↓	↑	↑	↑
[Trend]$_{\text{Theo}}$	↓	↑	↑	↑	↑	—	↓	↑	↑	↑

Table 2. Comparison between a phonon and a dislon. The topological constraint of a dislocation leads to a series of differences compared with a phonon, but still share many structural similarities between the two.

	Phonon	**Quantized dislocation (Dislon)**
Essence	small displacement **u**	displacement **u** with constraint $\oint d\mathbf{u} = -\mathbf{b}$
Mode expansion	$\mathbf{u}(\mathbf{R}) \sim \sum_{\mathbf{k}} u_{\mathbf{k}} \boldsymbol{\varepsilon}_{\mathbf{k}} e^{i\mathbf{k}\cdot\mathbf{R}}$	$\mathbf{u}(\mathbf{R}) \sim \sum_{\mathbf{k}} u_{\mathbf{k}} \mathbf{F}(\mathbf{k}) e^{i\mathbf{k}\cdot\mathbf{R}}$
Static limit	$\lim_{\mathbf{k}\to 0} u_{\mathbf{k}} = 0$	$\lim_{\kappa\to 0} u_{\mathbf{k}} = 1$
Electron-interaction	$H_{e-ph} = \sum_{\mathbf{k}'\mathbf{k}\sigma} g_{\mathbf{k}}^{ph} c_{\mathbf{k}'+\mathbf{k}\sigma}^{+} c_{\mathbf{k}'\sigma} (A_{\mathbf{k}} + A_{-\mathbf{k}}^{+})$	$H_{e-dis} = \sum_{\mathbf{k}'\mathbf{k}\sigma} g_{\mathbf{k}} c_{\mathbf{k}'+\mathbf{k}\sigma}^{+} c_{\mathbf{k}'\sigma} (a_{\mathbf{k}} + a_{-\mathbf{k}}^{+})$
Algebra	Bosonic $[A_{\mathbf{k}}, A_{\mathbf{k}'}^{+}] = \delta_{\mathbf{k}\mathbf{k}'}$	Two half-Bosons $[a_{\mathbf{k}}, a_{\mathbf{k}'}^{+}] = \delta_{\mathbf{k}\mathbf{k}'} \operatorname{sgn}(\mathbf{k})$

Coupling Constant with electron	$g_{\mathbf{k}}^{ph} = \frac{ieV_{\mathbf{k}}}{V}(\mathbf{k}\cdot\varepsilon_{\mathbf{k}})\sqrt{\frac{\hbar N}{2M\omega_{\mathbf{k}}}}$	$g_{\mathbf{k}} \equiv \frac{ieN}{VA}V_{\mathbf{k}}[\mathbf{k}\cdot\mathbf{F}(\mathbf{k})]\sqrt{\frac{\hbar N_D}{2m_{\mathbf{k}}\Omega_{\mathbf{k}}}}$
Effective Electron-electron interaction	$V_{eff}^{ph}(\mathbf{q}) = -\frac{\hbar\omega_{\mathbf{q}}\left\|g_{\mathbf{q}}^{ph}\right\|^2}{-\omega^2+\hbar^2\omega_{\mathbf{q}}^2}$	$V_{eff}(\mathbf{q}) = -\frac{\hbar\Omega_{\mathbf{q}}g_{\mathbf{q}}^{*}g_{\mathbf{q}}}{-\omega^2+\hbar^2\Omega_{\mathbf{q}}^2}$
Superconductivity	$\frac{1}{g_{ph}} = N(\mu)\int_0^{\omega_D}\frac{\tanh\left(\frac{\lambda(\xi)}{2T}\right)}{\lambda(\xi)}d\xi$	$\frac{1}{g_T} = N(\mu')\int_0^{\omega_D}\frac{\sum_{s=\pm1}\tanh\left(\frac{\lambda(\xi)+is\Gamma}{2T}\right)}{2\lambda(\xi)}d\xi$